JOURNAL OF OPTOELECTRONICS AND ADVANCED MATERIALS Vol. 12, No. 3, March 2010, p. 663 - 667

Influence of film thickness and optical constants on femtosecond laser-induced ablation of hydrogenated amorphous carbon films

R. KOTER, M. WEISE, A. HERTWIG, U. BECK, J. KRÜGER*
BAM Federal Institute for Materials Research and Testing, Division VI.4, Unter den Eichen 87, 12205 Berlin, Germany

Hydrogenated amorphous carbon layers were deposited on BK7 glass in a plasma-assisted chemical vapor deposition process. Low and high refracting films with thicknesses d ranging from 11 nm to 5.8 µm were produced having refractive indices n between 1.68 and 2.41 and linear absorption coefficients of α~100 cm^{-1} and α~20000 cm^{-1} at 800 nm wavelength as a result of different plasma modes. Laser ablation thresholds F_{th} in dependence on d were determined using 30-fs laser pulses. Low absorbing layers show a constant F_{th} while F_{th} increases with rising d up to the optical penetration depth of light α^{-1} for high absorbing films.

(Received June 18, 2009; accepted October 23, 2009)

Keywords: Physical radiation damage (61.80.-x), Laser-beam impact phenomena (79.20.Ds), Radiation treatment (81.40.Wx), Carbon (81.05.Uw), Optical constants (78.20.Ci)

1. Introduction

Hydrogenated amorphous carbon (a-C:H) layers have been used for several years as wear-resistant and low friction coatings for mechanical applications. As they offer a wide range of possible properties, they can be manufactured to endure high mechanical stress, to be biocompatible, self-lubricating and to show a specific surface energy [1,2].

A-C:H layers can be produced in a Plasma Assisted Chemical Vapor Deposition (PACVD) process from gaseous precursors (e.g. acetylene, methane). The properties of these layers primarily depend on the plasma conditions, which can be steered by various parameters like geometry of the plasma source, electrical settings of the plasma generation, as well as pressure and composition of the process gas. The ion energy within the plasma is influenced by the ionization potential of the precursor. Controlling this set of parameters, a large variety of layer properties such as hardness, modulus, and wear behavior can be tailored. It has previously been shown that mechanical and optical properties of different PACVD deposited a-C:H layers are correlated [3,4]. Therefore, optical methods like ellipsometry in the visible and infrared spectral region are qualified as film quality monitoring tools.

For mechanical applications of thin hard carbon layers, precise machining of those films is needed. Treatment with short laser pulses is one of the most precise and gentle methods to structure surfaces requiring detailed knowledge of the threshold energies of ablation/modification [5]. Furthermore, the tailoring of optical properties of a-C:H layers during the production process as well as their subsequent modification by laser radiation could open the possibility of a new type of carbon-based optics [6].

In the past, single pulse damage thresholds of a-C:H films on soda-lime glass were measured for 8 ns laser pulses at 532 nm wavelength and layer thicknesses between 60 nm and 13 µm. The light penetration depth amounted to 0.6 µm. The thickness of the films influenced the damage threshold. The threshold fluence reached the bulk value of 0.39 Jcm^{-2} for a layer thickness equal to the thermal diffusion length of 1.9 µm [7]. Furthermore, femtosecond laser experiments (120 fs, 620 nm) were performed with an a-C:H layer of 60 nm thickness on fused silica. Material removal and damage were attributed to fracture of the film as a result of relaxation of high internal stress of the pulsed laser deposition-grown film. A well-defined single pulse damage threshold of 0.25 Jcm^{-2} was reported [8]. For 150-fs laser ablation at 800 nm wavelength, a damage threshold of 0.16 Jcm^{-2} was found for diamond-like carbon (DLC) on silicon. An ablation rate of about 35 nm per pulse for a laser fluence of 0.4 Jcm^{-2} was observed [9]. Multi wavelength (539-1078 nm) studies utilizing different pulse durations (100 fs up to 150 ns) were done. A spallation effect was observed for a wide range of laser parameters [10]. The pulse duration influenced the quality of DLC laser processing significantly. Long laser pulses were not suitable for fine microprocessing [11]. Recently, a single pulse ablation threshold of about 2.5 Jcm^{-2} was published for 120-fs laser treatment (800 nm) of 630 nm thick DLC films on silicon [12].

The present study extends previous investigations with respect to different classes of samples (low and high absorbing carbon films), number of evaluated layer thicknesses (a total of 20 films) and laser parameters

(30 fs, 800 nm) significantly. Single and multi pulse ablation thresholds F_{th} of both film types vs. layer thickness d were measured. The results will be correlated to their optical constants.

2. Experimental

2.1 A-C:H film deposition

All layers were deposited in a plasma assisted chemical vapor deposition (PACVD) coating module (Roth & Rau) being part of a CS 730 ECS cluster coating system (VON ARDENNE). The module contains two plasma sources, an electron cyclotron resonance (ECR) microwave source and a radio frequency (RF) substrate bias source. Both sources can be used independently and in arbitrary combination of voltage and power. The process gas was a mixture of 40 sccm Acetylene and 20 sccm Argon. The pressure was 2.4×10^{-3} mbar for the ECR process, and 3.5×10^{-3} mbar for the RF process. All pure-RF samples were deposited with a voltage of 800 V substrate bias with a frequency of 13.56 MHz. All pure-ECR samples were deposited without substrate bias with a microwave antenna operating at 2.46 GHz. The microwave power was 800 W in all cases. The layer thickness of the amorphous carbon films was varied in a range from 11 nm to 5.8 µm by changing the processing time between 30 s and 3700 s. All samples were deposited on BK7 substrate disks (25 mm diameter, 5 mm thickness).

2.2 Ellipsometric characterization of the a-C:H layers

All ellipsometric measurements were carried out with a goniospectral ellipsometer M 2000 DI (J.A. Wollam). The instrument covers a wavelength range between 192 nm and 1692 nm with 710 distinctive wavelengths. All samples were measured at angles of incidence of 65°, 70°, and 75°, respectively. Ellipsometric data were analyzed with the WVASE32 software using an oscillator model based on a TAUC-LORENTZ-type peak function with LORENTZ-type sidebands added if necessary. In the case of thicker samples, the fitting procedure was corrected for surface roughness effects.

2.3 Laser ablation experiments

A femtosecond Ti:sapphire laser Femtopower Compact Pro (Femtolasers) was employed for the ablation experiments in air. 800-nm-central-wavelength pulses with 30 fs duration and pulse energies of up to 600 µJ were emitted at a repetition rate of 1 kHz. Pulse duration and spectrum were controlled by means of a dispersion-minimized autocorrelator (Femtolasers) and a spectrometer S2000 (Ocean Optics). Pulse energies were varied using a rotatable half-wave plate in front of the compressor unit and measured with a combination of photodiode and boxcar integrator (Stanford Research Systems). The energy calibration was done with a pyroelectric detector J25LP (Molectron). The laser beam profile was Gaussian.

The surface of each sample was positioned perpendicular to the direction of the incident laser beam. The laser beam was focused to $(1/e^2)$ spot diameters of about 160 µm. The number of laser pulses per spot was changed between 1 and 100.

The measurement of the diameters D of the laser-ablated areas was done with an optical microscope Eclipse L200 (Nikon). The Gaussian spot diameters and the ablation threshold fluences F_{th} were determined by a plot of D^2 vs. maximum pulse energy E_0 for a fixed number of pulses per spot [13,14].

3. Results and discussion

3.1 Optical constants of the a-C:H layers

Fig. 1 depicts a comparison of optical constants of an ECR-generated a-C:H layer and a RF-generated a-C:H layer. All ellipsometric results were modeled with a TAUC-LORENTZ-type absorption spectrum [15,16]. In the case of RF-generated layers, an additional LORENTZ oscillator was necessary to describe the broad absorption throughout the visible and the infrared spectral range. In both cases, the extinction coefficient k decreases in the near IR. In the case of the RF type layers, the significantly larger absorption peak is shifted to longer wavelengths and a much higher refractive index n is obvious compared to the ECR type samples. The ECR-generated specimens are transparent up to a thickness of several micrometers. The RF type samples appear black above a thickness of about 100 nm. At 800 nm wavelength, linear absorption coefficients of $\alpha\sim100$ cm^{-1} and $\alpha\sim20000$ cm^{-1} can be calculated for the ECR- and RF-generated films. While the light penetration depth of the ECR type a-C:H material is more than an order of magnitude larger than the thickest film, a light penetration depth (1/e length) of the RF type film of about 0.5 µm is evident. Bandgap energies of <1 eV (ECR type) and about 1.9 eV (RF type) were determined.

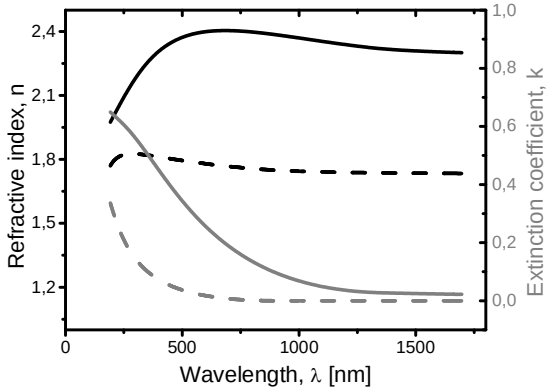

Fig. 1. Optical constants (n, k) vs. wavelength λ for a-C:H layers generated in RF and ECR plasma mode. Curves modeled from ellipsometry measurements. Black: refractive index n, grey: extinction coefficient k. Solid curves: RF sample, dashed curves: ECR sample.

The two types of a-C:H layers possess completely different mechanical properties in addition to the various optical constants. The ECR-generated layers generally exhibit a much lower hardness (H) and elastic modulus (M) than the RF type (typical values measured by instrumented indentation testing are for ECR type H=2 GPa, M=34 GPa, and for RF type H=34 GPa, M=336 GPa [4]). Furthermore, the content of hydrogen atoms in the ECR type is generally higher (>20 % vs. ~13 %). Therefore, the ECR-generated a-C:H layers are of the polymer-like type, while the RF-generated samples can be called diamond-like.

3.2 Laser ablation behavior

The different a:C-H films were illuminated using single (1-on-1) and multiple (10-on-1, 100-on-1) laser pulses per spot. For a fixed number of pulses per spot, varying pulse energies result in various diameters of the ablation craters. As an example, Figure 2 displays several ablation spots on a 62 nm thick high absorbing a-C:H layer.

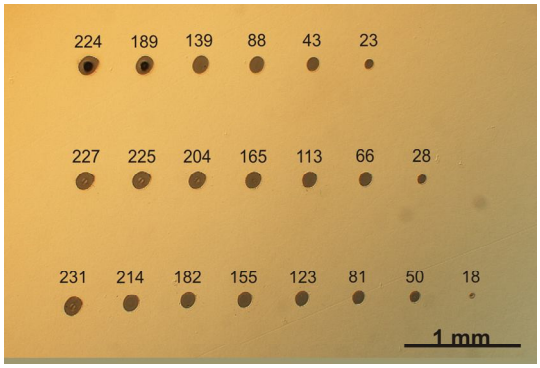

Fig. 2. Light-optical microscope micrograph of laser-ablated areas on a high absorbing a-C:H film (d=62 nm). Each row: Change of pulse energy for a constant number of pulses per spot. From the bottom up: 1-on-1, 10-on-1, and 100-on-1. Pulse energies (μJ) are indicated for the ablation spots.

The diameters of the ablated spots were measured microscopically. The squares of the crater diameters were plot vs. maximum pulse energy E_0 semi-logarithmically. Figure 3 shows a graph for a multi pulse treatment of a high absorbing layer. The ablation threshold energy E_{th} was obtained from the intersection point of the straight line with the E_0 axis. According to the relation [13,14]

$$D^2 = 2w^2 \ln\left(\frac{E_0}{E_{th}}\right), \qquad (1)$$

Gaussian beam radius w can be determined from the slope of the straight line. Here, values of E_{th}=20.7 μJ and w=89 μm were calculated. The corresponding ablation threshold fluence F_{th} can be obtained with the formula [14]

$$F_{th} = \frac{2E_{th}}{\pi w^2}. \qquad (2)$$

For multi pulse laser processing of the high absorbing a-C:H layer with a thickness of 127 nm, an ablation threshold of F_{th}=0.17 J/cm^2 was found.

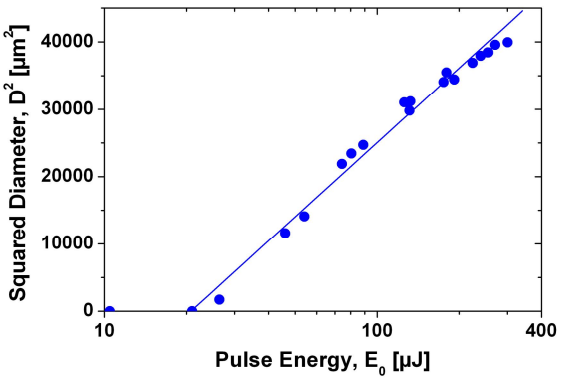

Fig. 3. Squared diameter vs. pulse energy for a 30-fs laser treatment of a high absorbing a-C:H film of 127 nm thickness. 10-on-1. Straight line: least-squares fit.

The ablation thresholds of single and multi pulse laser experiments on low absorbing (ECR-generated) and high absorbing (RF-generated) a-C:H layers are displayed in Figures 4 and 5, respectively. For the low absorbing films and a given number of pulses per spot, ablation threshold F_{th} does not change with film thickness d (Fig. 4) within the experimental uncertainty. The relative errors arise from the standard deviations of the fits according to equation (1) for the E_{th}- and w-calculation and the introduction of these values in equation (2). Indeed, an incubation behavior of F_{th} is observed. The multi pulse ablation threshold (100-on-1) is by a factor of two lower than the single pulse threshold (1-on-1). Obviously, absorbing defects (like graphitized areas [7]) are generated during repetitive illumination.

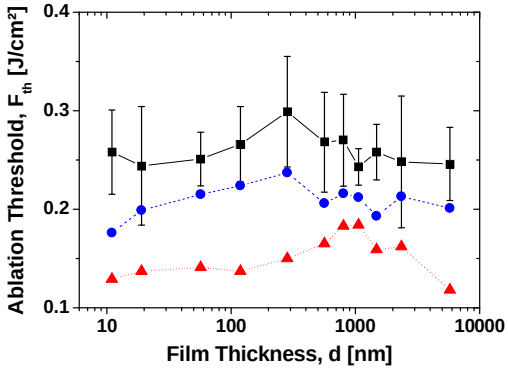

Fig. 4. Ablation threshold F_{th} vs. amorphous carbon film thickness d for layers with a low absorption coefficient. 1-on-1 (!, continuous line), 10-on-1 („, dashed line), and 100-on-1 (7, dotted line). The lines serve to guide the eye.

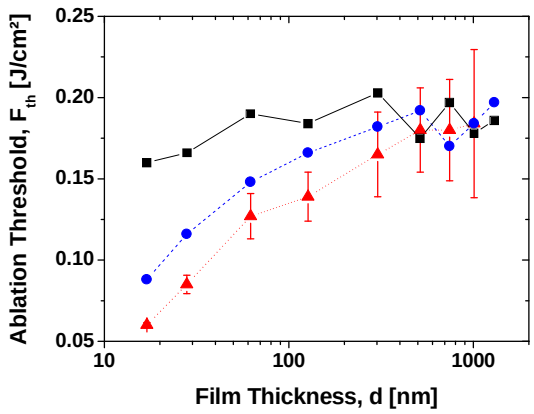

Fig. 5. Ablation threshold F_{th} vs. amorphous carbon film thickness d for layers with a high absorption coefficient. 1-on-1 (!, continuous line), 10-on-1 („, dashed line), and 100-on-1 (7, dotted line). The lines serve to guide the eye.

Fig. 5 depicts measurements of F_{th} vs. d for the high absorbing amorphous carbon films and single and multi pulse illumination conditions. In contrast to the low absorbing films, the damage threshold is found to increase with the layer thickness for films with a thickness below 500 nm. This layer thickness is comparable to the penetration depth of 800-nm light 1/α of about 500 nm for the high absorbing a-C:H films.

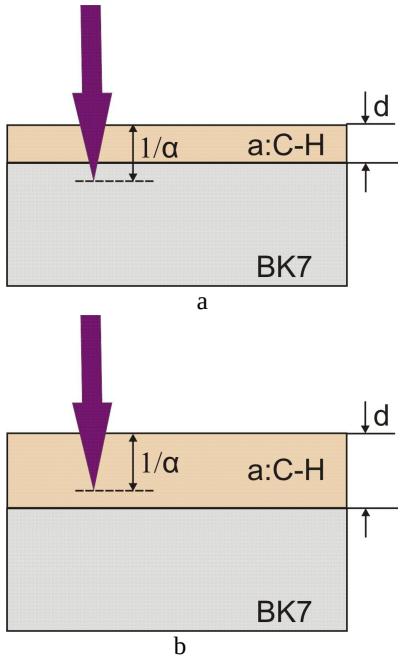

Fig. 6. Scheme of the relation between penetration depth of light 1/α and film thickness d for high absorbing layers with 1/α>d (a) and 1/α<d (b).

Fig. 6a shows the situation for thin absorbing films. The light penetration depth is larger than the layer thickness. In this regime, the ablation threshold increases with rising d up to 1/α≈d. At 1/α≈d, F_{th} reaches its bulk value and stays constant for 1/α<d (Fig. 6b). Hence, femtosecond laser-material interaction is different from the nanosecond case where F_{th} reached the bulk value for a layer thickness equal to the thermal diffusion length [7].

For low absorbing layers with a bandgap energy of 1.9 eV, F_{th} does not change with d in a thickness range from 11 nm to 5.8 µm. Taking into account the laser photon energy of 1.6 eV, two-photon absorption should be the dominant mechanism for energy coupling into the material. As a result of the nonlinear 30-fs laser-materials interaction, energy impact can be confined in a small layer of the order of 10 nm for laser fluences at the ablation threshold. This assumption is supported by the fact that ablation depths per pulse of 35 nm were published for a laser fluence of 0.4 Jcm^{-2} in the case of 150-fs laser treatment at 800 nm wavelength for a:C-H films. The authors determined the ablation rate as the ratio between layer thickness (0.9 µm) and number of pulses for a complete removal of the film [9].

4. Conclusions

Low and high absorbing amorphous carbon films with bandgap energies of 1.9 eV and <1 eV were deposited on BK7 glass substrates in a PACVD process using either ECR microwave or RF substrate bias plasma source, respectively. The samples in a thickness range between 11 nm and 5.8 µm were characterized ellipsometrically. Single and multi pulse laser ablation thresholds F_{th} of a:C-H layers in dependence on their thickness d were determined using 30-fs laser pulses at 800 nm wavelength (1.6 eV photon energy). F_{th} is not influenced by d for the low absorbing samples as a result of two-photon absorption with a strong energy confinement on a length scale of the order of 10 nm. For the linearly absorbing samples, F_{th} increases with rising d and equals the bulk value for a layer thickness of about 0.5 µm corresponding to the light penetration depth. Both sample types show a pronounced incubation behavior for multi pulse laser treatment.

References

[1] J. Robertson, Mater. Sci. Eng. R, **37**, 129 (2002).
[2] VDI 2840, Guideline: Carbon films – basic knowledge, film types and properties, 2005.
[3] D. P. Dowling, K. Donnelly, M. Monclus, M. McGuinness, Diamond and Related Materials **7**, 432 (1998).
[4] A. Hertwig, J. Krüger, M. Weise, U. Beck, Plasma Process. Polym., **4**, S76 (2007).
[5] D. Bäuerle, Laser Processing and Chemistry, Springer, Berlin, 3rd ed., 2000.

[6] A. Grigonis, A. Medvid, P. Onufrijevs, J. Babonas, A. Reza, Opt. Mater. **30**, 749 (2008).
[7] G. Daminelli, S. Pentzien, A. Hertwig, J. Krüger, Appl. Phys. A, **83**, 89 (2006).
[8] K. Sokolowski-Tinten, W. Ziegler, D. von der Linde, M. P. Siegal, D.L. Overmyer, Appl. Phys. Lett. **86**, 121911 (2005).
[9] G. Dumitru, V. Romano, H.P. Weber, S. Pimenov, T. Kononenko, M. Sentis, J. Hermann, S. Bruneau, Appl. Surf. Sci., **222**, 226 (2004).
[10] T. V. Kononenko, S. M. Pimenov, V. V. Kononenko, E. V. Zavedeev, V. I. Konov, G. Dumitru, V. Romano, Appl. Phys. A, **79**, 543 (2004).
[11] T. V. Kononenko, V. V. Kononenko, S. M. Pimenov, E. V. Zavedeev, V. I. Konov, V. Romano, G. Dumitru, Diamond and Related Materials, **14**, 1368 (2005).
[12] Y. Dong, H. Sakata, P. Molian, Appl. Surf. Sci. **252**, 352 (2005).
[13] J. M. Liu, Opt. Lett., **7**, 196 (1982).
[14] J. Bonse, J. M. Wrobel, J. Krüger, W. Kautek, Appl. Phys. A, **72**, 89 (2001).
[15] S. Logothetidis, Diamond Rel. Mater. **12**, 141 (2003).
[16] G. E. Jellison F. A. Modine, Appl. Phys. Lett. **69**, 371 (1996).

*Corresponding author: joerg.krueger@bam.de